AN EFFICIENT FITTED OPERATOR METHOD TO SOLVE DELAYED SINGULARLY PERTURBED DIFFERENTIAL-DIFFERENCE EQUATIONS

EIHAB B. M. BASHIER AND KAILASH C. PATIDAR

Department of Mathematics and Applied Mathematics, University of the
Western Cape, Private Bag X17, Bellville 7535, South Africa

ABSTRACT. Singularly perturbed second order differential-difference equations are well studied via asymptotic analysis by Lang and Miura [Singular perturbation analysis of boundary value problems for differential-difference equations, *SIAM Journal on Applied Mathematics* **42 (3)** (1982), 502–531; Singular perturbation analysis of boundary-value problems for differential-difference equations. V. Small shifts with layer behaviour, *SIAM Journal on Applied Mathematics* **54 (1)** (1994), 249–272; Singular perturbation analysis of boundary-value problems for differential-difference equations. VI. Small shifts with rapid oscillations, *SIAM Journal on Applied Mathematics* **54 (1)** (1994), 273–283]. Various attempts are made in the past to solve these problems numerically by making use of the Taylor series expansions of the delay terms which in turn imply that one is solving an approximate differential model rather than the original one. In this paper, we proposed a fitted numerical method which solves the original differential-difference equation directly. The proposed method is analyzed for convergence. Some numerical examples illustrating the theoretical observations are also presented.

Key Words: Singular perturbations; Boundary value problems; Delay differential equations; Fitted operator finite difference methods; Convergence; stability

AMS Subject Classification (2000): 34E15, 62P12, 65L10, 65L12, 65L20

1. Introduction

Boundary value problems (BVPs) of second order delay differential-difference equations (DDEs) model many biological systems. According to Lange and Miura [8], BVPs involving DDE are satisfied by the moments of the time of first exit [18] of temporally homogeneous Markov processes [14] governing such phenomena as the time between impulses of a nerve cell and the persistence times of populations with large random fluctuations.

Lange and Miura [11] stated that the determination of the expected time for the generation of action potentials in nerve cells (see, e.g., [1, 19]) by random synaptic inputs in the dendrites can be modelled as a first-exit time problem. They stated that

under particular circumstances the problem for the expected first exit-time y, given the initial membrane potential $x \in [x_1, x_2]$, can be formulated as a general boundary-value problem for a second order differential-difference equation of the form

$$(1.1) \quad \frac{\sigma^2}{2}\frac{d^2y}{dx^2} + (\mu - x)\frac{dy}{dx} + \lambda_E y(x + a_E) + \lambda_I y(x - a_I) - (\lambda_E + \lambda_I)y(x) = -1,$$

where the values $x = x_1$ and $x = x_2$ correspond to the inhibitory reversal potential and to the threshold value of the membrane potential for action potential generation, respectively. The first order term $-xy'$ corresponds to exponential decay between synaptic inputs whereas the undifferentiated terms correspond to excitatory and inhibitory synaptic inputs modelled as Poisson processes [7] with mean rates λ_E and λ_I, respectively, and produce jumps in the membrane potential of amounts a_E and $-a_I$, which are small quantities and could depend on voltage.

The above general singularly perturbed second order boundary value problem is considered by Lange and Miura in [11] and studied further by Kadalbajoo et al. in [6] and some of the references listed in [6]. Other relevant works include [8, 9, 10, 12].

The biological model stated by Lange and Miura in [11] leads us to consider a BVP for a singularly perturbed second order differential-difference equation [11]

$$(1.2) \qquad\qquad \varepsilon\frac{d^2y}{dx^2} + a(x)y(x - \delta) + b(x)y(x) = f(x), \ x \in [0, 1],$$

$$(1.3) \qquad\qquad y(\theta) = \varphi(\theta), \ \theta \in [-\delta, 0],$$

$$(1.4) \qquad\qquad y(1) = \gamma,$$

where γ is a real constant, $0 < \varepsilon \leq 1$ is the singular perturbation parameter, the functions $a(x)$, $b(x)$ and $f(x)$ are sufficiently smooth and the initial function $\varphi(x)$ is continuous.

If the shift parameter δ in (1.2) is taken to be zero (i.e., the case of no shift), then the solution of the resulting non-delayed problem can exhibit either a left or a right boundary layer depending on whether the function $a(x)$ is positive or negative in the interval $[0, 1]$. For very small values of the shift $\delta > 0$, the solution profile can still maintain the existing boundary layer. Once the shift parameter start increasing, small oscillations start appearing in the boundary layer region. After some stage when these oscillations grow, the boundary layer is completely destroyed and oscillations dominate throughout the region. This particular feature makes this problem more interesting because the such change in the overall dynamics can not be resolved by many fitted mesh methods. We overcome this difficulty by using a fitted operator method instead.

Lange and Miura [11] reduced the DDE (1.2) into a system of ODEs of the form

$$\varepsilon y_n''(x) + a(x)y_n'(x) + b(x)y_n(x) = f(x) + a(x)(y_{n-1}'(x) - y_{n-1}'(x - \delta))$$

and used an iterative algorithm to solve the resulting problem. Their simulations show both boundary layer behaviour (for small shifts) and oscillatory dynamics (for large shifts).

Patidar and Sharma [16] considered problem (1.2) with small shifts. They used a two term Taylor expansion to approximate problem (1.2) through a non-delayed singularly perturbed second order differential equation. They separated the cases of left and right boundary layers and constructed ε-uniformly convergent fitted operator finite difference methods for solving the approximate problem.

Rather than solving an approximate problem (the one obtained by using Taylor expansions) as in Patidar and Sharma [16], here we develop a numerical method that can solve the problem (1.2)–(1.4) directly.

The rest of this paper is organized as follows. In Section 2, we discuss some of the qualitative properties of the solution of (1.2)–(1.4). The fitted operator finite difference method is constructed in Section 3. In Section 4, we analyze this method. Numerical examples are presented in Section 5. Finally, in Section 6, we discuss these numerical results.

2. **Qualitative behaviour of the solution**

In this section, we review the qualitative behaviour of the solution of (1.2)–(1.4) based on the work found in [11].

If the shift δ is taken to be zero in (1.2)–(1.4), then the resulting ordinary differential equation will have either a boundary layer at the left side ($x = 0$) or a boundary layer at the right side ($x = 1$), depending on whether $a(x) > 0$ or $a(x) < 0$, respectively.

Letting the delay parameter δ taking very small values will not affect the boundary layer initially. Then increasing the value of δ leads to the appearance of oscillations within the boundary layer without destroying its structure. Increasing the value of δ further, oscillations (starting from the layer side) begin to dominate until the boundary layer is destroyed completely and they simultaneously move towards the other end. These features have been shown via some figures in [11]. Their simulations indicate how significant effects of the delay on the first order derivative.

Some notable observations from [11] is as follows:

1. In the case of no delay (i.e., when $\delta = 0$) with $a(x) > 0$, there is a boundary layer at $x = 0$, and the outer solution is given by

$$y(x) = \gamma e^{\int_x^1 b(t)/a(t)dt} + \mathcal{O}(\varepsilon).$$

The analytical solution in this case is then given by

$$y(x) = \Gamma + (\phi(0) - \Gamma)e^{-a(0)x/\varepsilon} + \mathcal{O}(\varepsilon),$$

where $\Gamma = \gamma e^{\int_x^1 b(t)/a(t)dt}$.

2. For $\delta = \tau\varepsilon$ where τ is a positive parameter of $\mathcal{O}(1)$, they assumed an outer solution of the form

$$y(x) = \sum_{j=0}^{\infty} y_j(x)\varepsilon^j,$$

as $\varepsilon \to 0$, where y_0 satisfies the reduced problem obtained by setting $\varepsilon = 0$, with boundary condition $y_0(1) = \gamma$, whereas the functions $y_j(x), j = 1, 2, \ldots$ satisfy equations of the form

$$\varepsilon y_j''(x) + a(x)y'(x - \delta) + b(x)y(x) = a(x)\sum_{k=1}^{j}(-1)^k\frac{\tau^k}{k!}y_{j-k}^{(k+1)}(x) - y''(x),$$

with boundary conditions

$$y_j(1) = 0.$$

Using the change in the variables $\widetilde{x} = x/\varepsilon$ and $\widetilde{y}(\widetilde{x}) = y(\varepsilon x)$, the solution of the transformed problem

$$\widetilde{y}'' + a(\varepsilon\widetilde{x})\widetilde{y}'(\widetilde{x} - \tau) + \varepsilon b(\varepsilon\widetilde{x})\widetilde{y}(\widetilde{x}) = 0, \ 0 \leq \widetilde{x} \leq \infty,$$

can be written as

$$\widetilde{y}(\widetilde{x}) = \sum_{j=1}^{\infty} \widetilde{y}_j(\widetilde{x})\varepsilon^j,$$

where the smooth component $\widetilde{y}_0(\widetilde{x})$ satisfies the problem

$$\widetilde{y}_0''(\widetilde{x}) + \widetilde{y}_0'(\widetilde{x} - \tau) = 0, \ \widetilde{y}_0(\widetilde{x}) = 1 \text{ on } [-\tau, 0].$$

Integrating the above, we obtain

$$\widetilde{y}'(\widetilde{x}) + \widetilde{y}(\widetilde{x} - \tau) = \widetilde{y}'(0) + 1 = \Gamma,$$

assuming that $a(0) = 1$.

The solution of the above problem is obtained by first applying the Laplace transformation to both sides of the above problem, which yields

$$\widetilde{Y}_0(s) = \frac{1}{s} + \frac{\Gamma - 1}{s(s + e^{-\tau s})}$$

and then one uses the inverse Laplace transform.

The transformed problem has infinite number of poles. One of the poles is $s = 0$ and the other poles are obtained by finding the roots of

$$P(s, \tau) = s + e^{-s\tau} = 0.$$

The results about the poles of $P(s, \tau)$ are summarized as follows,

(a) For $\tau \in (0, e^{-1})$, there are two distinct real roots $s_0 \in (-\infty, -e)$ and $s_1 \in (-e, -1)$. When $\tau \to 0^+$, then $s_0 \to -\infty$ and $s_1 \to -1$, whereas when $\tau > 0$, all the other roots occur in complex conjugate pairs with $Re(s_n) \approx (1/\tau)\ln(2\tau/(4n - 3)\pi)$ as $n \to \infty$.

(b) For $\tau = e^{-1}$, the two negative roots coalesce at $s_1 = -e$.

(c) For $\tau > e^{-1}$, the roots split into complex conjugate pairs, and at $\tau = \pi/2$, $Re(s_1) = 0$.

(d) For $\tau > \pi/2$, s_1 and $\bar{s}_1$ cross the imaginary axis to the right half plane.

Then the solution obtained by the inversion of $\widetilde{Y}_0(s)$ is given by

$$\widetilde{y}_0(\widetilde{x}) = \Gamma + c_0 e^{s_0 \widetilde{x}} + c_1 e^{s_1 \widetilde{x}} + \sum_{n=2}^{\infty} (c_n e^{s_n \widetilde{x}} + \bar{c}_n e^{s_n \widetilde{x}}),$$

where

$$c_n = \frac{\Gamma - 1}{s_n(1 + \tau s_n)}, \quad n = 0, 1, \ldots.$$

From the natures of the poles of the transformed problem, Lange and Miura [11] concluded that

(a) for $\tau \in (0, e^{-1})$, the roots s_0 and s_1 are real and distinct, and

$$\widetilde{y}_0(\widetilde{x}) \approx \Gamma + c_0 e^{s_0 \widetilde{x}} + c_1 e^{s_1 \widetilde{x}}, \quad \widetilde{x} \to \infty, \quad \varepsilon \to 0,$$

is an accurate numerical approximation for the boundary layer solution $\widetilde{y}(\widetilde{x})$.

(b) for $\tau > e^{-1}$, s_0 and s_1 are complex conjugates, and c_0 and s_0 are replaced by $\bar{c}_1$ and $\bar{s}_1$.

(c) the leading order layer solution neither depends on the function $b(x)$ nor on the function $f(x)$, except through Γ.

The qualitative information described above will be useful for verification of the numerical results that we obtain by the fitted method presented in next section.

3. Construction of the numerical method

In this section, we design a fitted numerical method to solve the problem (1.2)–(1.4).

To begin with, we partition the interval $[0, 1]$ through the points

$$x_0 = 0 < x_1 < \cdots < x_N = 1,$$

where N is a positive integer and $x_{m+1} - x_m = h = 1/N$ for $m = 0, \ldots, N - 1$.

The value of N is chosen in such a way that $\delta = sh$ for some positive integer s. This will make it possible for the shift parameter δ to coincide with the grid point x_s. This is in line with most of the works seen in the literature (see, e.g., [2, 3, 17]) for this kind of problems where either the length of the interval is considered as the multiple of the delay parameter or both the interval length and the delay are integer multiples of the step-size h.

Using the theory of difference equations (see, e.g., [13, 15]), the appropriate denominator function (ϕ_m^2) in the discretization of (1.2)–(1.4) can be considered as

$$(3.1) \qquad \phi_m^2 = \begin{cases} \frac{h\varepsilon}{a_m}\left(e^{\frac{ha_m}{\varepsilon}} - 1\right), & \text{if } a_m < 0, \\[2mm] \frac{h\varepsilon}{a_m}\left(1 - e^{-\frac{ha_m}{\varepsilon}}\right), & \text{if } a_m > 0, \\[2mm] \frac{4}{\rho_m^2}\sinh^2\frac{\rho_m h}{2}, & \text{if } a_m = 0 \text{ and } b_m > 0, \\[2mm] \frac{4}{\rho_m^2}\sin^2\frac{\rho_m h}{2}, & \text{if } a_m = 0 \text{ and } b_m < 0, \end{cases}$$

where

$$\rho_m = \sqrt{\frac{b_m}{\varepsilon}}.$$

At the grid points x_m, the second order derivative term in the equation (1.2) is approximated as

$$\left.\frac{d^2 y}{dx^2}\right|_{x=x_m} \approx \frac{y_{m+1} - 2y_m + y_{m-1}}{\phi_m^2}.$$

Similarly, the first order term involving delay is approximated at $x_m - \delta$ as

$$\left.\frac{dy}{dx}\right|_{x=x_m-\delta} \approx \frac{y(x_{m+1} - \delta) - y(x_m - \delta)}{h}.$$

Using the above approximations, we obtain the following difference method for (1.2):

$$(3.2) \qquad \varepsilon\frac{y_{m+1} - 2y_m + y_{m-1}}{\phi_m^2} + a_m\frac{y(x_{m+1} - \delta) - y(x_m - \delta)}{h} + b_m y_m = f_m,$$

$m = 1, \ldots, N - 1$.

Equation (3.2) can be further simplified to

$$(3.3) \quad \frac{\varepsilon}{\phi_m^2}y_{m-1} + \left(b_m - \frac{2\varepsilon}{\phi_m^2}\right)y_m + \frac{\varepsilon}{\phi_m^2}y_{m+1} + \frac{a_m}{h}y(x_{m+1} - x_s) - \frac{a_m}{h}y(x_m - x_s) = f_m,$$

$m = 1, \ldots, N - 1$

For $m \le s$, the delayed term $y(x_m - \delta)$ is evaluated from the history function as

$$y(x_m - \delta) = \varphi(x_m - \delta) = \varphi(x_m - x_s),$$

and therefore, equation (3.3) becomes

$$(3.4) \quad \frac{\varepsilon}{\phi_m^2}y_{m-1} + \left(b_m - \frac{2\varepsilon}{\phi_m^2}\right)y_m + \frac{\varepsilon}{\phi_m^2}y_{m+1} = f_m - \frac{a_m}{h}\varphi(x_{m+1} - x_s) - \frac{a_m}{h}\varphi(x_m - x_s),$$

when $m < s$, whereas when $m = s$, we have

$$(3.5) \qquad \frac{\varepsilon}{\phi_s^2}y_{s-1} + \left(b_s - \frac{2\varepsilon}{\phi_s^2}\right)y_s + \frac{\varepsilon}{\phi_s^2}y_{s+1} + \frac{a_{s+1}}{h}y_1 = f_s - \frac{a_s}{h}\varphi(0).$$

For $m = s + 1, \ldots, N - 1$, equation (3.3) takes the form

$$(3.6) \quad \frac{\varepsilon}{\phi_m^2}y_{m-1} + \left(b_m - \frac{2\varepsilon}{\phi_m^2}\right)y_m + \frac{\varepsilon}{\phi_m^2}y_{m+1} + \frac{a_m}{h}y(x_{m+1-s}) - \frac{a_m}{h}y(x_{m-s}) = f(x_m).$$

Our fitted operator finite difference method consists of equation (3.3) along with the initial data (1.3) and the boundary condition (1.4).

Combining (3.4), (3.5) and (3.6), we obtain a linear system

$$AY = F,$$

where A is the $(N-1) \times (N-1)$ matrix

$$A_{j,k} = \begin{cases} -\frac{2\varepsilon}{\phi_m^2} + b_m, & \text{if } j = k = m, \ m = 1, \ldots, N-1 \\ \frac{\varepsilon}{\phi_{m-1}^2} & \text{if } j = m-1, \ k = m, \ m = 2, \ldots, N-1 \\ \frac{\varepsilon}{\phi_m^2}, & \text{if } j = m, \ k = m-1, \ m = 2, \ldots, N-1 \\ \frac{a_s}{h}, & \text{if } j = s \text{ and } k = 1 \\ -\frac{a_m}{h}, & \text{if } j = m-s, \ k = m, \ m > s \\ \frac{a_m}{h}, & \text{if } j = m-s+1, \ k = m, \ m > s \\ 0, & \text{otherwise.} \end{cases}$$

The $N-1$ entries of the right hand side vector F are given by

$$F_m = \begin{cases} f(x_1) - \frac{\varepsilon}{\phi_1^2} y(x_0) - \frac{a_1}{h}(\varphi(x_2 - \delta) - \varphi(x_1 - \delta)), & \text{if } m = 1, \\ f_m - \frac{a_m}{h}(\varphi(x_{m+1} - \delta) - \varphi(x_m - \delta)) & \text{if } 1 < m < s, \\ f_s + \frac{a_s}{h} y_0, & \text{if } m = s, \\ f_m, & \text{if } s < m < N-1, \\ f_{N-1} - \frac{\varepsilon}{\phi_{N-1}^2} \gamma, & \text{if } m = N-1, \end{cases}$$

and Y denotes the vector $[y_1, \ldots, y_{N-1}]^T$ of unknowns.

4. Analysis of the numerical method

In this section, we analyze the proposed fitted method. We will consider the case of large delays that are sufficient to destroy the boundary layer. In this case, highly oscillatory solutions will be obtained. Therefore, we assume that the solution function $y(x)$ and its derivatives up to order three are bounded by a constant C, which is independent of ε. On the other hand, the cases of the small delays have already been analyzed by other researchers in the past, see, e.g., [6], where due to the smallness of the delay, the differential equation (obtained via Taylor approximations) was still a very good approximation of the problem (1.2)–(1.4).

Convergence of the method: The local truncation error of the method at $x = x_m$ is given by

$$\text{LTE} = \varepsilon \left(y''(x_m) - \frac{y(x_{m+1}) - 2y(x_m) + y(x_{m-1})}{\phi_m^2} \right)$$

(4.1)
$$+ a_m \left(y'(x_m - \delta) - \frac{y(x_{m+1} - \delta) - y(x_m - \delta)}{h} \right),$$

which implies that

$$|\text{LTE}| \le \varepsilon \left| y''(x_m) - \frac{y(x_m + h) - 2y(x_m) + y(x_m - h)}{\phi_m^2} \right|$$

$$(4.2) \qquad + |a_m| \left| y'(x_m - \delta) - \frac{y(x_{m+1} - \delta) - y(x_m - \delta)}{h} \right|.$$

The first term on the right hand side of the inequality (4.2) can be replaced by

$$\varepsilon \left(y''(x_m) - \frac{y(x_{m+1}) - 2y(x_m) + y(x_{m-1})}{h^2} \right)$$

$$(4.3) \qquad + \varepsilon \left(\frac{y(x_{m+1}) - 2y(x_m) + y(x_{m-1})}{h^2} - \frac{y(x_{m+1}) - 2y(x_m) + y(x_{m-1})}{\phi_m^2} \right).$$

This gives

$$\varepsilon \left| y''(x_m) - \frac{y(x_{m+1}) - 2y(x_m) + y(x_{m-1})}{h^2} \right| = \mathcal{O}(h^2) \to 0 \text{ as } h \to 0$$

Now, by expanding ϕ_m^2, we see that

$$\varepsilon \left| \frac{y(x_{m+1}) - 2y(x_m) + y(x_{m-1})}{h^2} - \frac{y(x_{m+1}) - 2y(x_m) + y(x_{m-1})}{\phi_m^2} \right|$$

$$\le \frac{\varepsilon \mathcal{O}(\frac{h}{\varepsilon})}{1 + \mathcal{O}(\frac{h}{\varepsilon})} \to 0 \text{ as } h \to 0,$$

provided that $h \le C\delta$, where $C \in (0, 1]$ is a constant.

The second term on the right hand side of the inequality (4.2) satisfies

$$|a_m| \left| y'(x_m - \delta) - \frac{y(x_{m+1} - \delta) - y(x_m - \delta)}{h} \right| \le |a_m|\mathcal{O}(h) \to 0 \text{ as } h \to 0.$$

Hence, the LTE is $\mathcal{O}(h)$ and it tends to zero as $h \to 0$, which proves that the method is convergent of order 1.

Remark 4.1. In order to accommodate all the delays, it is reasonable to take the step-size of the magnitude of δ. Hence, the condition $h \le C\delta$ for the convergence is logically very appropriate.

Stability of the method: We would like to determine the conditions on the step-size h, under which the proposed fitted method is stable. The stability of our method depends on the eigenvalues of the matrix A denoted by λ_m, $m = 1, \ldots, N - 1$. If for all $m = 1, \ldots, N - 1$, the eigenvalues of A^{-1} denoted by λ_m^{-1} satisfy

$$|\lambda_m^{-1}| < 1,$$

then the method will be stable.

We make use of the Gershgorin's disk theorem [5], which states that each eigenvalue λ_m of the matrix A should lie in a Gershgorin's disk (denoted by D_m), which is centered at $b_m - 2\varepsilon/\phi_m^2$ and has a radius equals to the magnitude of the summation

of the non-diagonal elements in row m. Our strategy here is to consider each Gershgorin's disk D_m, and let the whole disk lies in $(-\infty, -1)$ one time and lies in $(1, \infty)$ another time and for each of the two cases we determine the range for the step-size h which allow the disk to lie in the corresponding region. This is done by allowing both the left and right bounds of the disk to lie together either in $(-\infty, -1)$ or in $(1, \infty)$.

For $m = 1, \ldots, s-1$, each Gershgorin's disk is centered at $b_m - 2\varepsilon/\phi_m^2$ and have a radius $2\varepsilon/\phi_m^2$, that is

$$D_m = \left[b_m - \frac{4\varepsilon}{\phi_m^2}, b_m \right].$$

Then, $|\lambda_m^{-1}| < 1$ if $|\lambda_m| > 1$ and this will happen only if both the limits of D_m are either below -1 or both are above 1.

If we solve the two inequalities

$$b_m < -1$$

and

$$b_m - \frac{4\varepsilon}{\phi_m^2} < -1,$$

we obtain

$$h < \frac{\varepsilon}{a_m} W \left(\frac{4a_m^2}{b_m + 1} \right), \quad \text{for } a_m > 0$$

and

$$h < \frac{2a_m^2}{b_m + 1}, \quad \text{for } a_m < 0,$$

where $W(x)$ denotes the Lambert W function evaluated at x.

On the other hand, if we solve the two inequalities

$$b_m > 1$$

and

$$b_m - \frac{4\varepsilon}{\phi_m^2} > 1,$$

we obtain

$$h < \frac{\varepsilon}{a_m} W \left(\frac{4a_m^2}{b_m - 1} \right), \quad \text{for } a_m > 0$$

and

$$h < \frac{2a_m^2}{b_m - 1}, \quad \text{for } a_m < 0.$$

The Gershgorin's disk D_s is given by

$$D_s = \left[b_s - \frac{4\varepsilon}{\phi_m^2} - \frac{a_{s+1}}{h}, b_m + \frac{a_{s+1}}{h} \right]$$

and again $|\lambda_s| > 1$ only if both the limits of D_s are below -1 or both are above 1.

The solution of the inequalities

$$b_s - \frac{4\varepsilon}{\phi_m^2} - \frac{a_{s+1}}{h} < -1$$

and

$$b_m + \frac{a_{s+1}}{h} < -1,$$

leads to

$$h < \frac{\varepsilon}{a_s} W \left(\frac{4a_s^2}{b_s + 1} \right), \text{ for } a_s > 0$$

and

$$h < \frac{2a_s^2}{b_s + 1}, \text{ for } a_s < 0,$$

whereas the solution of the inequalities

$$b_s - \frac{4\varepsilon}{\phi_m^2} - \frac{a_{s+1}}{h} > 1$$

and

$$b_m + \frac{a_{s+1}}{h} > 1,$$

leads to

$$h < \frac{\varepsilon}{a_s} W \left(\frac{4a_s^2}{b_s - 1} \right), \text{ for } a_s > 0$$

and

$$h < \frac{2a_s^2}{b_s - 1}, \text{ for } a_s < 0.$$

Similarly, for $m = s + 1, \ldots, N - 1$, the Gershgorin's disks are given by

$$D_m = \left[b_m - \frac{4\varepsilon}{\phi_m^2} - \left(\frac{a_{m+1}}{h} - \frac{a_m}{h} \right), b_m + \left(\frac{a_{m+1}}{h} - \frac{a_m}{h} \right) \right],$$

and the eigenvalues λ_m in this case satisfy $|\lambda_m| > 1$ only if both the limits of D_m are below -1 or both are above 1.

By solving the inequalities

$$b_m - \frac{4\varepsilon}{\phi_m^2} - \left(\frac{a_{m+1}}{h} - \frac{a_m}{h} \right) < -1$$

and

$$b_m + \left(\frac{a_{m+1}}{h} - \frac{a_m}{h} \right) < -1,$$

we obtain

$$h < \frac{\varepsilon}{a_m} W \left(\frac{4a_m^2}{b_m + 1} \right), \text{ for } a_m > 0$$

and

$$h < \frac{2a_m^2}{b_m + 1}, \text{ for } a_m < 0.$$

On the other hand, if we solve the two inequalities

$$b_m - \frac{4\varepsilon}{\phi_m^2} - \left(\frac{a_{m+1}}{h} - \frac{a_m}{h} \right) > 1$$

and

$$b_m + \left(\frac{a_{m+1}}{h} - \frac{a_m}{h} \right) > 1,$$

we obtain

$$h < \frac{\varepsilon}{a_m} W \left(\frac{4a_m^2}{b_m - 1} \right), \text{ for } a_m > 0$$

and

$$h < \frac{2a_m^2}{b_m - 1}, \text{ for } a_m < 0.$$

The above condition on h guarantee the stability of the method. It should be noted that due to the nature of the coefficients, none of the above conditions seem to be severe.

5. Numerical results

Example 5.1 ([11])**.** We consider (1.2)–(1.4) with $a(x) = b(x) = \varphi(x) = \gamma = 1$, $f(x) = 0$.

Example 5.2 ([11])**.** We consider (1.2)–(1.4) with $\varphi(x) = 1$, $a(x) = b(x) = \gamma = -1$ and $f(x) = 0$.

In Figure 1, we plot the solutions for Example 5.1 corresponding to different values of the delay. These plots show different dynamics: left boundary layers, oscillations on the layer side and movement of the oscillations to the other side. In Figure 2, we plot the solutions for Example 5.2 for different values of δ. These plots also show different behaviour for the solution of the system, including smooth and oscillatory behaviour. These numerical results confirm the observations made earlier about the qualitative behaviour of the solution.

In tables 1, 3 and 2, 4 we tabulate maximum errors and convergence rates corresponding to examples 5.1 and 5.2, respectively. We see from these results that the proposed method produces parameter uniform numerical results and is first order convergent. This agrees with the theoretical rate of convergence as discussed in Section 4. From tables 1 and 2, we see that the numerical method is convergent with $\mathcal{O}(h)$, which does agree with the convergence analysis in Section 4. In tables 5-8, we show the errors and convergence rates, obtained by fixing the parameter ϵ to the value 0.05 and varying δ in the range $[0.02, 0.2]$, for examples 5.1 and 5.2. We again see that the performance of the method is unaffected.

6. Concluding remarks

In this paper, we developed a fitted numerical method for solving a second order delay differential equation with a delay involved in the first order derivative term. The method is shown to be stable and convergent.

By applying the fitted method to Example 5.1, we noticed that for very small values of the delay δ (up to $\delta = 0.5\varepsilon$), the left boundary layer is maintained. When the
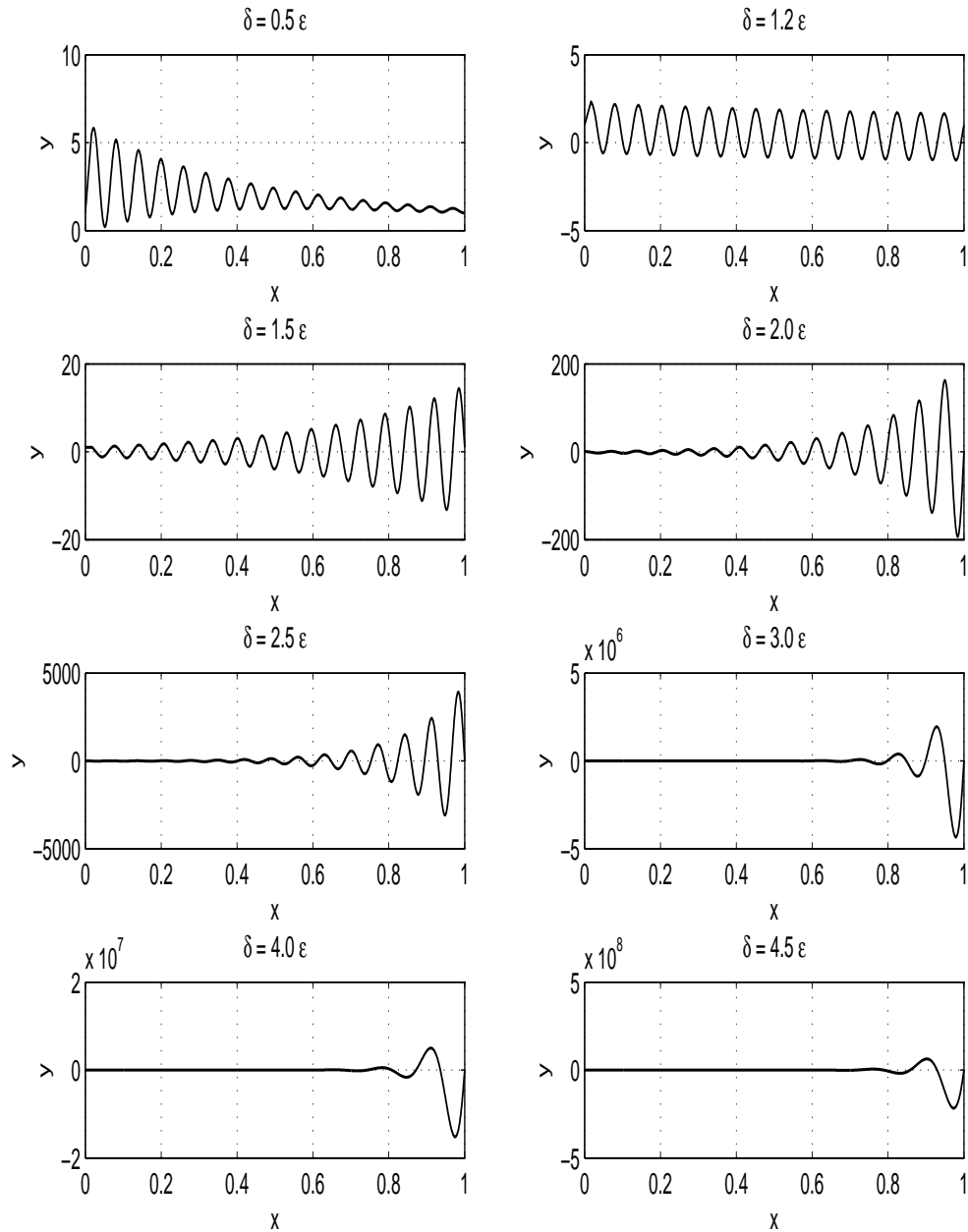
FIGURE 1. Solutions for Example 5.1, with $a(x) = b(x) = \varphi(x) = \gamma = 1$ and $f(x) = 0$.

delay is more than 0.5ε but remains below $\delta = 1.1\varepsilon$, oscillations within the boundary layer region are seen while the layer structure is still being maintained. For delays that are greater than 1.1ε, the oscillations begin to dominate in the boundary layer region and the shape of the boundary layer is completely destroyed when the value of the delay parameter reaches 1.5ε. At around $\delta = 1.6\varepsilon$ the oscillations profile is
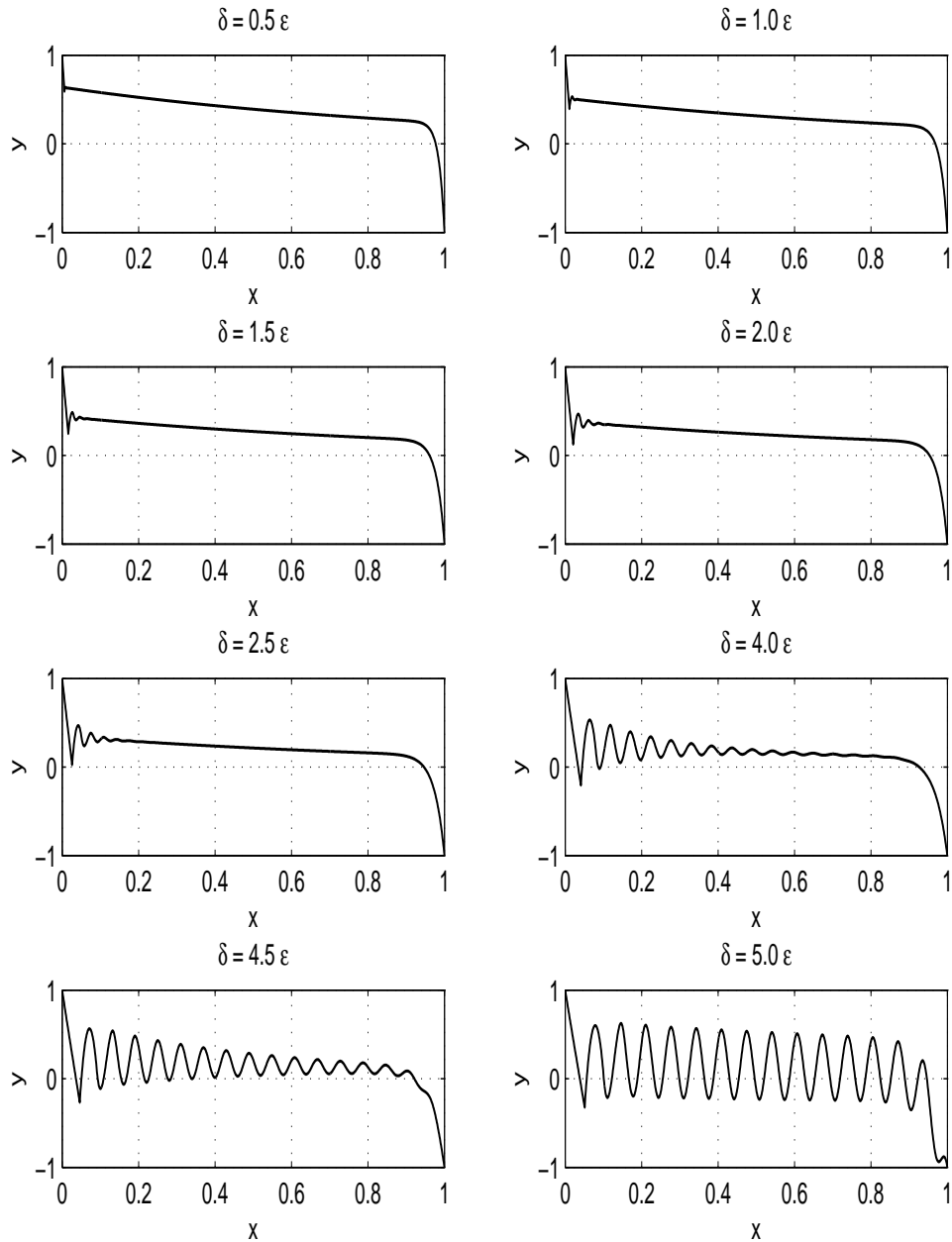
FIGURE 2. Solutions for Example 5.2, $\varphi(x) = 1$, $a(x) = b(x) = \gamma = -1$ and $f(x) = 0$.

same on the left and right sides. After that the oscillations become weaker on the left side than on the right side and their magnitudes on the right side grow rapidly by increasing the value of the delay. The profile remains like that for the rest of the values of the delay. It should be noted that the results which we obtain by our fitted numerical method for this example agree with those found in [11].

TABLE 1. Maximum errors (using double mesh principle [4]) for Example 5.1; $\delta = 0.05$.

ε	$n = 8$	$n = 16$	$n = 32$	$n = 64$	$n = 128$	$n = 256$
10^{-1}	1.548×10^{-2}	8.380×10^{-3}	4.298×10^{-3}	2.176×10^{-3}	1.094×10^{-3}	5.484×10^{-4}
10^{-3}	9.071×10^{-3}	4.778×10^{-3}	2.450×10^{-3}	1.239×10^{-3}	6.229×10^{-4}	3.123×10^{-4}
10^{-5}	9.032×10^{-3}	4.757×10^{-3}	2.440×10^{-3}	1.234×10^{-3}	6.202×10^{-4}	3.109×10^{-4}
10^{-7}	9.032×10^{-3}	4.757×10^{-3}	2.440×10^{-3}	1.234×10^{-3}	6.201×10^{-4}	3.109×10^{-4}
10^{-9}	9.032×10^{-3}	4.757×10^{-3}	2.440×10^{-3}	1.234×10^{-3}	6.201×10^{-4}	3.109×10^{-4}
10^{-11}	9.032×10^{-3}	4.757×10^{-3}	2.440×10^{-3}	1.234×10^{-3}	6.201×10^{-4}	3.109×10^{-4}
10^{-13}	9.032×10^{-3}	4.757×10^{-3}	2.440×10^{-3}	1.234×10^{-3}	6.201×10^{-4}	3.109×10^{-4}
10^{-15}	9.032×10^{-3}	4.757×10^{-3}	2.440×10^{-3}	1.234×10^{-3}	6.201×10^{-4}	3.109×10^{-4}

TABLE 2. Convergence rates r_k of the numerical method for Example 5.1 for $n_k = 8 \times 2^k, k = 1(1)5; \delta = 0.05$.

ε	r_1	r_2	r_3	r_4	r_5
10^{-1}	0.96	0.98	0.99	1.00	1.00
10^{-3}	0.96	0.98	0.99	1.00	1.00
10^{-5}	0.96	0.98	0.99	1.00	1.00
10^{-7}	0.96	0.98	0.99	1.00	1.00
10^{-9}	0.96	0.98	0.99	1.00	1.00
10^{-11}	0.96	0.98	0.99	1.00	1.00
10^{-13}	0.96	0.98	0.99	1.00	1.00
10^{-15}	0.96	0.98	0.99	1.00	1.00

TABLE 3. Maximum errors (using double mesh principle [4]) for Example 5.2; $\delta = 0.05$.

ε	$n = 8$	$n = 16$	$n = 32$	$n = 64$	$n = 128$	$n = 256$
10^{-1}	3.445×10^{-2}	1.884×10^{-2}	9.853×10^{-3}	5.041×10^{-3}	2.550×10^{-3}	1.282×10^{-3}
10^{-3}	5.301×10^{-2}	2.972×10^{-2}	1.580×10^{-2}	8.144×10^{-3}	4.136×10^{-3}	2.084×10^{-3}
10^{-5}	5.328×10^{-2}	2.988×10^{-2}	1.589×10^{-2}	8.192×10^{-3}	4.160×10^{-3}	2.097×10^{-3}
10^{-7}	5.329×10^{-2}	2.989×10^{-2}	1.589×10^{-2}	8.192×10^{-3}	4.161×10^{-3}	2.097×10^{-3}
10^{-9}	5.329×10^{-2}	2.989×10^{-2}	1.589×10^{-2}	8.192×10^{-3}	4.161×10^{-3}	2.097×10^{-3}
10^{-11}	5.329×10^{-2}	2.989×10^{-2}	1.589×10^{-2}	8.192×10^{-3}	4.161×10^{-3}	2.097×10^{-3}
10^{-13}	5.329×10^{-2}	2.989×10^{-2}	1.589×10^{-2}	8.192×10^{-3}	4.161×10^{-3}	2.097×10^{-3}
10^{-15}	5.329×10^{-2}	2.989×10^{-2}	1.589×10^{-2}	8.192×10^{-3}	4.161×10^{-3}	2.097×10^{-3}

The solutions for Example 5.2 are explained in Figure 2. Again we see the movement from very smooth profiles corresponding to very small delays to oscillatory profile with small oscillations to oscillatory dynamics.

Tables 1, 3, 2 and 4 show that the order of convergence for the proposed numerical method is $\mathcal{O}(h)$ and this agrees with the convergence analysis discussed in Section 4.

TABLE 4. Convergence rates r_k of the numerical method for Example 5.2 for $n_k = 8 \times 2^k$, $k = 1(1)5$; $\delta = 0.05$.

ε	r_1	r_2	r_3	r_4	r_5
10^{-1}	0.94	0.97	0.98	0.99	1.00
10^{-3}	0.91	0.96	0.98	0.99	0.99
10^{-5}	0.91	0.96	0.98	0.99	0.99
10^{-7}	0.91	0.96	0.98	0.99	0.99
10^{-9}	0.91	0.96	0.98	0.99	0.99
10^{-11}	0.91	0.96	0.98	0.99	0.99
10^{-13}	0.91	0.96	0.98	0.99	0.99
10^{-15}	0.91	0.96	0.98	0.99	0.99

TABLE 5. Maximum errors (using double mesh principle [4]) for Example 5.1; $\epsilon = 0.05$.

δ	$h = \delta/4$	$h = \delta/8$	$h = \delta/16$	$h = \delta/32$	$h = \delta/64$	$h = \delta/128$
0.2	2.207×10^{-2}	1.176×10^{-2}	6.074×10^{-3}	3.088×10^{-3}	1.557×10^{-3}	7.817×10^{-4}
0.18	2.121×10^{-2}	1.125×10^{-2}	5.801×10^{-3}	2.946×10^{-3}	1.484×10^{-3}	7.451×10^{-4}
0.16	2.068×10^{-2}	1.094×10^{-2}	5.631×10^{-3}	2.857×10^{-3}	1.439×10^{-3}	7.222×10^{-4}
0.14	2.043×10^{-2}	1.079×10^{-2}	5.547×10^{-3}	2.812×10^{-3}	1.416×10^{-3}	7.106×10^{-4}
0.12	1.902×10^{-2}	9.994×10^{-3}	5.122×10^{-3}	2.594×10^{-3}	1.305×10^{-3}	6.546×10^{-4}
0.10	1.716×10^{-2}	8.955×10^{-3}	4.575×10^{-3}	2.312×10^{-3}	1.162×10^{-3}	5.828×10^{-4}
0.08	1.535×10^{-2}	7.956×10^{-3}	4.051×10^{-3}	2.044×10^{-3}	1.027×10^{-3}	5.147×10^{-4}
0.06	1.284×10^{-2}	6.607×10^{-3}	3.352×10^{-3}	1.688×10^{-3}	8.473×10^{-4}	4.244×10^{-4}
0.04	9.894×10^{-3}	5.052×10^{-3}	2.553×10^{-3}	1.283×10^{-3}	6.434×10^{-4}	3.221×10^{-4}
0.02	5.733×10^{-3}	2.900×10^{-3}	1.458×10^{-3}	7.312×10^{-4}	3.662×10^{-4}	1.832×10^{-4}

TABLE 6. Convergence rates r_k of the numerical method for Example 5.1 for $h = \delta/2^{k+1}$, $k = 1(1)5$; $\epsilon = 0.05$.

δ	r_1	r_2	r_3	r_4	r_5
0.2	0.91	0.95	0.98	0.99	0.99
0.18	0.91	0.96	0.98	0.99	0.99
0.16	0.92	0.96	0.98	0.99	0.99
0.14	0.92	0.96	0.98	0.99	0.99
0.12	0.93	0.96	0.98	0.99	1.00
0.10	0.94	0.97	0.98	0.99	1.00
0.08	0.95	0.97	0.99	0.99	1.00
0.06	0.96	0.98	0.99	0.99	1.00
0.04	0.97	0.98	0.99	1.00	1.00
0.02	0.98	0.99	1.00	1.00	1.00

The condition that the step-size must be below the singular perturbation parameter looks very severe, but the fact that the delay and the singular perturbation parameter are of similar order shows that this condition is reasonable. This is not

TABLE 7. Maximum errors (using double mesh principle [4]) for Example 5.2; $\epsilon = 0.05$.

δ	$h = \delta/4$	$h = \delta/8$	$h = \delta/16$	$h = \delta/32$	$h = \delta/64$	$h = \delta/128$
0.20	2.068×10^{-2}	1.094×10^{-2}	5.631×10^{-3}	2.857×10^{-3}	1.439×10^{-3}	7.222×10^{-4}
0.18	2.013×10^{-2}	1.062×10^{-2}	5.459×10^{-3}	2.767×10^{-3}	1.393×10^{-3}	6.992×10^{-4}
0.16	1.842×10^{-2}	9.664×10^{-3}	4.951×10^{-3}	2.506×10^{-3}	1.261×10^{-3}	6.324×10^{-4}
0.14	1.838×10^{-2}	9.641×10^{-3}	4.936×10^{-3}	2.497×10^{-3}	1.256×10^{-3}	6.300×10^{-4}
0.12	1.653×10^{-2}	8.607×10^{-3}	4.393×10^{-3}	2.219×10^{-3}	1.115×10^{-3}	5.592×10^{-4}
0.10	1.535×10^{-2}	7.956×10^{-3}	4.051×10^{-3}	2.044×10^{-3}	1.027×10^{-3}	5.147×10^{-4}
0.08	1.351×10^{-2}	6.967×10^{-3}	3.538×10^{-3}	1.783×10^{-3}	8.949×10^{-4}	4.483×10^{-4}
0.06	1.135×10^{-2}	5.815×10^{-3}	2.944×10^{-3}	1.481×10^{-3}	7.430×10^{-4}	3.721×10^{-4}
0.04	8.380×10^{-3}	4.264×10^{-3}	2.151×10^{-3}	1.080×10^{-3}	5.412×10^{-4}	2.709×10^{-4}
0.02	4.733×10^{-3}	2.389×10^{-3}	1.200×10^{-3}	6.015×10^{-4}	3.011×10^{-4}	1.506×10^{-4}

TABLE 8. Convergence rates r_k of the numerical method for Example 5.2 for $h = \delta/2^{k+1}, k = 1(1)5; \epsilon = 0.05$.

δ	r_1	r_2	r_3	r_4	r_5
0.20	0.92	0.96	0.98	0.99	0.99
0.18	0.92	0.96	0.98	0.99	0.99
0.16	0.93	0.96	0.98	0.99	1.00
0.14	0.93	0.97	0.98	0.99	1.00
0.12	0.94	0.97	0.99	0.99	1.00
0.10	0.95	0.97	0.99	0.99	1.00
0.08	0.96	0.98	0.99	0.99	1.00
0.06	0.96	0.98	0.99	1.00	1.00
0.04	0.97	0.99	0.99	1.00	1.00
0.02	0.99	0.99	1.00	1.00	1.00

surprising because even the MATLAB *dde23* solver has been designed to include the time delay δ, 2δ and 3δ on the mesh in order for *dde23* not to avoid the step-sizes smaller than or equal to δ.

Moreover, if we consider the first example, where $\varepsilon = 0.01$, $a = b = 1$ and remembering that $\delta = \mathcal{O}(\varepsilon)$, then the restriction on the step-size h which is computed from the Lambert W function is $h < 0.0393$ which is absolutely reasonable.

The proposed approach is very simplistic in nature and hence we can easily extend it to solve the higher order problems in this class.

REFERENCES

[1] A. Bahra and K. Cikurel, *Neurology*, Elsevier Health Sciences, 1999.
[2] K. Cooke, P. van den Driessche and X. Zou, Interaction of maturation delay and nonlinear birth in population and epidemic models, *Journal of Mathematical Biology* **39** (1999), 332–352.

[3] R. V. Culshaw and S. Ruan, A delay-differential equation model of HIV infection of CD4$^+$T-cells, *Mathematical Biosciences* **165** (2000), 27-39.

[4] E. P. Doolan, J. J. H. Miller and W. H. A. Schilders, *Uniform Numerical Methods for Problems with Initial and Boundary Layers*, Boole Press, Dublin, 1980.

[5] R. A. Horn and C. R. Johnson, *Matrix Analysis*, Cambridge University Press, 1990.

[6] M. K. Kadalbajooa, K. C. Patidar and K. K. Sharma, ε-Uniformly convergent fitted methods for the numerical solution of the problems arising from singularly perturbed general DDEs, *Applied Mathematics and Computation* **182(1)** 2006, 119–139.

[7] J. F. C. Kingman, *Poisson processes*, Oxford University Press, 1993.

[8] C. G. Lange and R. M. Miura, Singular perturbation analysis of boundary value problems for differential-difference equations, *SIAM Journal on Applied Mathematics* **42 (3)** (1982), 502–531.

[9] C. G. Lange and R. M. Miura, Singular perturbation analysis of boundary-value problems for differential-difference equations II. Rapid oscillations and resonances, *SIAM Journal on Applied Mathematics* **45 (5)** (1985), 687–707.

[10] C. G. Lange and R. M. Miura, Singular perturbation analysis of boundary-value problems for differential-difference equations III. Turning point problems, *SIAM Journal on Applied Mathematics* **45 (5)** (1985), 708–734.

[11] C. G. Lange and R. M. Miura, Singular perturbation analysis of boundary-value problems for differential-difference equations. V. Small shifts with layer behaviour, *SIAM Journal on Applied Mathematics* **54 (1)** (1994), 249–272.

[12] C. G. Lange and R. M. Miura, Singular perturbation analysis of boundary-value problems for differential-difference equations. VI. Small shifts with rapid oscillations, *SIAM Journal on Applied Mathematics* **54 (1)** (1994), 273–283.

[13] J. M.-S. Lubuma and K. C. Patidar, Contributions to the theory of non-standard finite difference methods and applications to singular perturbation problems, Advances in the Applications of Nonstandard Finite Difference Schemes, R.E. Mickens (editor), World Scientific, Singapore, 2005, 513–560.

[14] M. B. Marcus and J. Rosen, *Markov processes, Gaussian processes and local times*, Cambridge University Press, 2006.

[15] K. C. Patidar and K. K. Sharma, Uniformly convergent nonstandard finite difference methods for singularly perturbed differential-difference equations with delay and advance, *International Journal for Numerical Methods in Engineering* **66(2)** (2006), 272–296.

[16] K. C. Patidar and K. K. Sharma, ε-Uniformly convergent non-standard finite differece methods for singularly perturbed differential-difference equations with small delay, *Applied Mathematics and Computation* **175** (2006), 864–890.

[17] J. W. H. So, J. Wu and Y. Yang, Numerical steady state and Hopf bifurcation analysis on the diffusive Nicholson's blowflies equation, *Applied Mathematics and Computation* **111** (2000), 33–51.

[18] H. C. Tukwell, On the first exit time problem for temporally homogeneous Markov processes, Journal of Applied Probability **13** (1976), 39–48.

[19] P. H. Young and P. A. Young, *Basic Clinical Neuroscience*, Lippincott Williams & Wilkins, 2007.